

ULRR

Optimising the multiplicative AF model parameters for AA7075 cyclic plasticity and fatigue simulation

Item Type	Article
Authors	Agius, Dylan J.;Kajtaz, Mladenko;Kourousis, Kyriakos I.;Wallbrink, Chris;Hu, Weiping
Citation	Aircraft Engineering and Aerospace Technology;90 (2), pp. 251-260
Publisher	Emerald Group Publishing Ltd.
Download date	2026-05-20 22:46:05
Item License	https://creativecommons.org/licenses/by-nc-sa/1.0/
Link to Item	https://hdl.handle.net/10344/6858

Optimising the multiplicative AF model parameters for AA7075 cyclic plasticity and fatigue simulation

Dylan Agius¹, Mladenko Kajtaz¹, Kyriakos I. Kourousis^{2,1*}, Chris Wallbrink³ and Weiping Hu³

¹School of Engineering, RMIT University, Melbourne, Victoria 3000, Australia

²School of Engineering, University of Limerick, Limerick, Co. Limerick, Ireland

³Defence Science and Technology Group, 506 Lorimer St, Port Melbourne, Victoria 3207, Australia

*Corresponding Author Email: kyriakos.kourousis@ul.ie

Abstract

Purpose - This study presents the improvements of the Multicomponent Armstrong-Frederick model with Multiplier performance through a numerical optimisation methodology available in a commercial software. Moreover, it explores the application of a multi-objective optimisation technique for the determination of the parameters of the constitutive models using uniaxial experimental data gathered from Aluminium Alloy 7075-T6 specimens. This approach aims to improve the overall accuracy of stress-strain response, not only for symmetric strain controlled loading but also for asymmetrically strain- and stress- controlled loading.

Design/methodology/approach - Experimental data from stress and strain controlled symmetric and asymmetric cyclic loadings have been utilised for this purpose. The analysis of the influence of the parameters on simulation accuracy has led to an adjustment scheme that can be used for focused optimisation of the MAFM model performance. The method was successfully employed to provide a better understanding of the influence of each model parameter on the overall simulation accuracy.

Findings - The optimisation identified an important issue associated with competing ratcheting and mean stress relaxation objectives; highlighting the issues with arriving at a parameter set that can simulate ratcheting and mean stress relaxation for load cases not reaching at complete relaxation.

Post-print: Dylan Agius, Mladenko Kajtaz, Kyriakos I. Kourousis, Chris Wallbrink, Weiping Hu, (2018) "Optimising the multiplicative AF model parameters for AA7075 cyclic plasticity and fatigue simulation", Aircraft Engineering and Aerospace Technology, Vol. 90 Issue: 2, pp.251-260, <https://doi.org/10.1108/AEAT-05-2017-0119>

Practical implications - The study uses a strain-life fatigue application to demonstrate the importance of incorporating a technique such as the presented multi-objective optimisation method to arrive at robust parameters capable of accurately simulating a variety of transient cyclic phenomena.

Originality/value - The proposed methodology improves the accuracy of cyclic plasticity phenomena and strain-life fatigue simulations for engineering applications. This study is considered a valuable contribution for the engineering community, as it can act as starting point for further exploration of the benefits that can be obtained through material parameter optimisation methodologies for models of the Multicomponent Armstrong-Frederick class.

Keywords: Cyclic plasticity; Fatigue; Kinematic hardening; Mean stress relaxation; Optimisation; aircraft structures.

Introduction

The application of advanced kinematic hardening models of cyclic plasticity can significantly improve the simulation accuracy, due to their ability to account for the effect of transient cyclic phenomena such as mean stress relaxation and ratcheting. Simulation accuracy is important for many engineering applications, particularly for fatigue life calculation of structures containing notches (Hu and Wallbrink, 2014). The motivation behind this is that a combination of strain and stress controlled loading occurs at the notch root, where localised plasticity is present (Hu et al., 1999). This highlights the importance of accuracy in simulating these two cyclic phenomena. Consequently, it is crucial that the parameters defining the plasticity model are determined accurately.

As the experimental understanding of materials increases, so has the level of sophistication and complexity of elastoplastic models, leading to increased parameter calculation requirements, as recognised by Grama et al. (2015). In order to improve the calculation process of elastoplastic constitutive model parameters, various optimisation techniques have been investigated, with two main optimisation strategies identified, the gradient-based (Mahnken and Stein, 1996, Saleeb et al., 2002, Desai and Chen, 2006) and the genetic algorithm (GA) methodologies (Rahman et al., 2005, Krishna et al., 2009, Badnava et al., 2012, Agius et al., 2017a, Mahmoudi et al., 2011, Farrahi et al., 2014, Rokouzzaman and Sakai, 2010, Khademi et al., 2015, Cermak et al., 2015, Zhao and Lee, 2002, Khutia and Dey, 2014, Franulović et al., 2009). As highlighted by Furukawa et al. (2002), the disadvantage of the gradient-based approach in constitutive model parameter determination lies in the solution divergence, an issue not typically associated with GA methodologies, which are instead associated with poor solution efficiency. Therefore, a combination of the two strategies has also been applied in the past (e.g. Chaparro et al., 2008) to improve the parameter optimisation process, while further improved optimisation strategies have also been suggested and investigated by other researchers (Sinaie et al., 2014, Yun and Shang, 2011).

This study explores the application of a multi-objective optimisation technique for the determination of the parameters of the constitutive models using uniaxial experimental data gathered from Aluminium Alloy (AA) 7075-T6 specimens. Since this study aims to simulate

cyclic transient effects of two different control methods of varying amplitudes (strain and stress), the difficulty at arriving at a parameter set capable of achieving accurate simulations of both phenomena justifies the application of a robust optimisation strategy, such as the GA, so as to limit the potential of solution divergence. This approach aims to improve the overall accuracy of stress-strain response, not only for symmetric strain controlled loading but also for asymmetrically strain- and stress- controlled loading. Moreover, this analysis aims to shed light on how the parameter values obtained from commonly used methodologies can be adjusted to improve the simulation results. Finally, the study uses a strain-life fatigue application to demonstrate the importance of incorporating a technique such as the presented multi-objective optimisation method to arrive at robust parameters capable of accurately simulating a variety of transient cyclic phenomena.

Cyclic plasticity model

In the rate independent plasticity theory, the fundamental components of a constitutive model include a yield criterion, a flow rule, and a kinematic, isotropic or combined hardening rule. In this work, the von Mises yield criterion and an associative flow rule were used, as appropriate for ductile metals. The Multicomponent Armstrong-Frederick model with Multiplier (MAFM) (Dafalias et al., 2008) was the kinematic hardening rule implemented in this study, due to its proven ability to simulate cyclic transient effects of aluminium alloys (Kourousis and Dafalias, 2013, Agius et al., 2017b). The MAFM is based on the widely used Multicomponent Armstrong-Frederick (Armstrong and Frederick, 1966) model (MAF) (Chaboche et al., 1979), with the difference between them being in the way hardening is modelled.

The uniaxial formulation of the MAF model is given in Eq. 1, where X_i is the back-stress, c_i and γ_i are the material parameters and $d\varepsilon^p$ is the incremental plastic strain. The MAFM model has a fourth term as given Eq. 2, in addition to the three terms given by Eq. 1. The square brackets in Eq. 2 contain the so-called multiplier expressed in a non-dimensional back-stress X^* which itself is given in Eq. 3, where C^* and γ^* are also material parameters.

For $i = 1,3$:

$$dX_i = C_i d\varepsilon^p - \gamma_i X_i |d\varepsilon^p| \quad (1)$$

For $i = 4$:

$$dX_i = \left[\gamma_i + \gamma_i^* \left(\frac{C_i^*}{\gamma_i^*} - X_i^* \right) \right] \left(\frac{C_i}{\gamma_i} d\varepsilon^p - X_i |d\varepsilon^p| \right) \quad (2)$$

$$dX_i^* = C_i^* d\varepsilon^p - \gamma_i^* X_i^* |d\varepsilon^p| \quad (3)$$

Furthermore, an isotropic hardening rule, as proposed by Chaboche (Chaboche, 1986), is given in Eq. 4, where R is the magnitude of the yield stress and R_s , b the material parameters controlling its evolution.

$$dR = b(R_s - R) |d\varepsilon^p| \quad (4)$$

Parameter determination methodology

The parameter determination methodology presented in the next sub-sections is composed of two steps, de-termination of the baseline parameters using one of the established methods, and the optimisation of these parameters.

Baseline parameters

The initial parameter calculation method is described in the work of Dafalias et al. (2008) and it is based on the methodology originally developed by Chaboche (1991) for the Multicomponent Armstrong-Frederick with Threshold (MAF-T) model (Chaboche, 1991). The formulation of the first three back-stresses is given by Eq. 1. Explicitly integrating Eq. 1 and assuming the initial conditions of the loading branch are given as $X_0 = -C_i/\gamma_i$ and $\varepsilon^{p0} = -\varepsilon^{p0}$, Eq. 5 can be used in conjunction with the loading branch of a saturated hysteresis loop (Bari and Hassan, 2000). The values of C_i and γ_i were determined by fitting Eq. 5 to the 1.8% strain-controlled stabilised cycle obtained from AA 7075-T6 experiments. The MAFM model parameters were adjustment with the technique outlined in (Dafalias et al., 2008), previously tested for AA 7050 (Kourousis and Dafalias, 2013). The obtained parameters are summarised in Table 1.

$$\sigma = \sigma_y + \sum_{i=1}^4 \frac{C_i}{\gamma_i} \left(1 - 2 \exp\left(\gamma_i \left(\varepsilon^p - (-\varepsilon^{p0})\right)\right)\right) + R \quad (5)$$

Table 1. Baseline MAFM parameters for AA7075-T6.

Elasticity Modulus, E (MPa)		69,000	
Yield Strength, σ_{yield} (MPa)		376	
C_1 (MPa)	330,000	γ_1	2,505
C_2 (MPa)	8,050	γ_2	202
C_3 (MPa)	2,849	γ_3	15
C_4 (MPa)	1,000	γ_4	100
C_4^*/γ_4^*	13.2	γ_4^*	0.05
R_s (MPa)	16	b	5

Optimising Parameters

The parameter optimisation methodology consists of coupling the MAFM material model with an optimisation engine provided by the commercial software package modeFrontier (ESTECO, 2015). In the applied optimisation workflow, there are three common sections for a typical problem: input, processing, and constraints and objectives. In total, 13 input parameters were used, with each attributed an allowable range as shown in Table 2. Although the yield stress is a material constant, it was allowed to vary in the optimisation process to improve the shape of the hysteresis loop by avoiding sharp and unrealistic elastic to plastic transition.

Table 2. Ranges and objectives for optimisation.

Parameters	Range	Objective	Objective Loads (Max, Min)
σ_{yield} (MPa)	(250,380)	Hysteresis loop shape	(1.8%, -1.8%)
C_1, C_2, C_3, C_4 (MPa)	(1,10 ⁵)	Ratcheting	(540MPa,-460MPa)
$\gamma_1, \gamma_2, \gamma_3, \gamma_4$	(1,10 ⁵)		(530MPa,-440MPa)
γ_4^*	(1,10 ⁶)		(510MPa,-430MPa)
C_4^*/γ_4^*	(1,10 ⁶)	Mean stress relaxation	(1.55%,-0.05%)
R_s (MPa)	(0,65)		(1.60%, 0.20%)
b	(0,10 ⁵)		(1.90%,-0.10%)

A schematic of the optimisation workflow employed in this study is given in Fig. 1. Each stage of the workflow is outlined in the corresponding sections. Although the primary focus of this study is on the MAFM model, the optimisation workflow presented can also be applied to other elastoplastic constitutive models, through the following modifications:

- Modification of the initial population stage to include different parameter strings to recognise the alternate model formulation;
- Modification of the elastoplastic constitutive model stage to include the elastoplastic constitutive models required for the investigation.

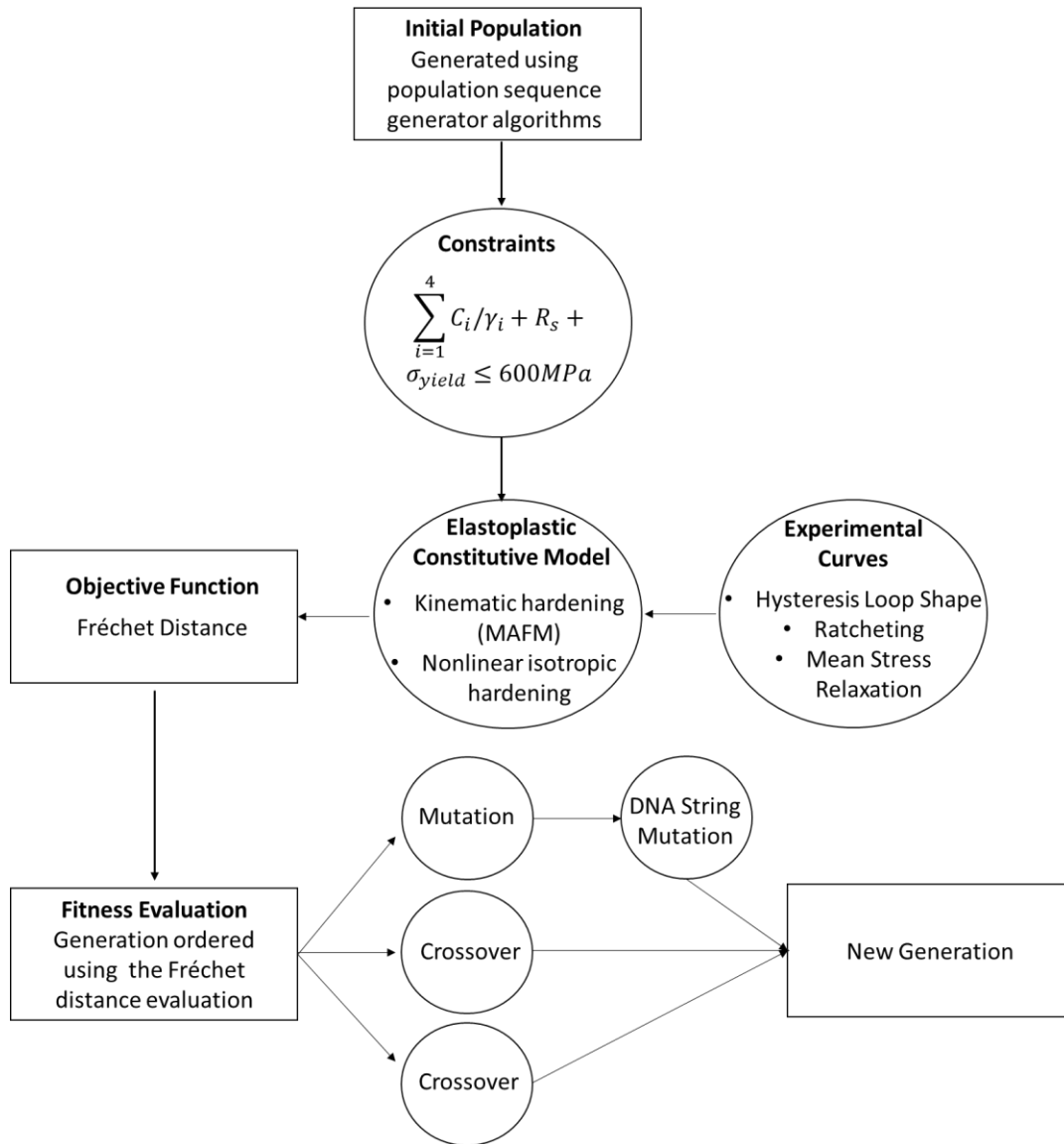


Fig. 1 Schematic representation of the optimisation workflow utilised.

Initial Population

The first stage of the optimisation workflow requires the formation of an initial population of 25 parameters. Strings of parameter values were determined by selecting from the ranges outlined in Table 2 using one or a combination of pseudo random sequence generator, which in this study was the Sobol sequence. An additional restriction was imposed on the parameter selection process to ensure that the parameters selected did not deviate significantly from the maximum stress attained under symmetric strain-controlled tests (Eq. 6). A relatively large value of

600MPa was used as the maximum bound to exclude unrealistic solutions for the parameters and to avoid putting too much restriction on the search space for the parameters. A slight error in the approximation of the hysteresis loop shape is tolerated to ensure greater opportunity at reaching reasonable accuracy for other types of material behaviour (e.g. ratcheting).

$$\sum_{i=1}^4 C_i / \gamma_i + R_S + \sigma_{yield} \leq 600MPa \quad (6)$$

Objective Function

The input parameters which form the generation were then used to integrate the MAFM model using a backward Euler scheme, in conjunction with the nonlinear isotropic hardening model. The outputs of the simulation were compared to experimentally collected data to determine the accuracy of the selected parameters. The objectives of the optimisation workflow were used to minimise fitness values based on the difference between normalised simulated outputs and experimental data for ‘objective loads’ given in Table 2, which correspond to the stabilised hysteresis loop shape, the mean stress relaxation rate and the ratcheting rate. Moreover, a number of different loading cases were used to ensure that the optimised parameters were able to simulate effectively a diverse set of load cases.

The fitness value was defined according to the Fréchet distance (Alt and Godau, 1995), which is the maximum Euclidean distance of all possible ways to traverse the simulated and experimental curves. The Fréchet distance (FD) can be calculated using Eq. 7, where P and Q refer to the functions of the two curves being compared and i and j refer to points along those curves.

$$FD[i, j] = \max \left[\|P(i) - Q(j)\|, \min \left(FD[i-1, j-1], FD[i, j-1], FD[i-1, j] \right) \right] \quad (7)$$

The obtained fitness scores were then submitted to the optimiser, which would generate a new set of values.

Optimiser

To concurrently achieve multiple objectives, a proprietary version of Multi-Objective Genetic Algorithm (MOGA-II) (ESTECO, 2015) was used as the optimisation engine in this study, which is a modified version of the MOGA (Poloni and Pediroda, 1997). As with the classical MOGA, the MOGA-II is based on a natural selection and genetics concept, whereby at the end of each optimisation iteration, the population of test parameter strings (or parameter sets) were evaluated to form a new population based on the best performing (with respect to the defined objectives) parameter strings. The new population consists of elite children, crossover children, and mutation children ('children' refers to a new parameter string, developed from previous parameter strings, or 'parent' strings). The children are formed from the combination of parent parameter strings, consequently, the next population will contain parameters selected from previous iterations. However, mutation children are formed from a random modification of a parent string, which demonstrates that the next population will also include new untested parameter strings. In MOGA-II, the amount by which the parent string is mutated can be set using DNA String Mutation Ratio. The MOGA-II settings used in this study are given in Table 3.

Table 3. MOGA-II settings used in the multi-objective study.

Population		Selection Probability	Crossover Probability	Mutation	
Size	Algorithm			Probability	DNA String Mutation Ratio
25	Sobol	0.1	0.5	0.2	0.05

Optimised Parameters

The values of the MAFM parameters obtained from the optimisation method are provided in Table 4. Due to the nature of a multi-objective study, a number of possible solutions exist; however, in this study, selection of the most suitable parameter set is that based on attempting to achieve parameter robustness. The selected values in Table 4 corresponded to the solution which provided a relatively balanced accuracy across the different elastoplastic features considered in the optimisation (hysteresis loop shape, mean stress relaxation, strain ratcheting).

Table 4. Optimised MAFM parameters for AA7075-T6.

Elasticity Modulus, E (MPa)		69,000	
Yield Strength, σ_{yield} (MPa)		302	
C_1 (MPa)	58,016	γ_1	55,740
C_2 (MPa)	43,437	γ_2	43,757
C_3 (MPa)	370	γ_3	370
C_4 (MPa)	465	γ_4	465
C_4^*/γ_4^*	513,447	γ_4^*	703,641
R_s (MPa)	51	b	34

Results

Uniaxial simulations

In order to determine the accuracy of the optimised parameters, symmetric/asymmetric strain controlled and asymmetric stress controlled simulations were conducted and compared to simulations using the baseline parameters. Error calculations using Eq. 8, where M refers to the number of data points used in the comparison, were used as a means of comparing the accuracy of the base-line and optimised parameter outputs, with values given in Table 5.

$$Error = \frac{1}{M} \sum_{i=1}^M \left(\frac{Y_i^{EXP} - Y_i^{SIM}}{Y_{MAX}^{EXP}} \right)^2 \quad (8)$$

Out of the seven load cases examined (four strain controlled and three stress controlled) an improvement was achieved in the five (from modest to drastic improvement) for the optimized simulations. A slight and very modest deterioration was observed for the (1.5%, -1.5%) and (1.65%, 0.05%) strain loading cases (-0.27% and -4.11% respectively). Overall, the improvement achieved, as measured by the average error across all cases, was very significant (81.74%), which provides an indicator of the optimisation process effectiveness.

Table 5. Error calculation for each simulation for both baseline and optimised simulations.

Loading condition	Baseline Simulations (%)	Optimised Simulations (%)	Improvement with Optimised simulations (%)
(1.5%, -1.5%)	0.01	0.28	<i>-0.27</i>
(1.35%, 0.05%)	65.17	7.42	+57.75
(1.60%, 0.20%)	38.10	8.99	+29.11
(1.65%, 0.05%)	9.92	14.03	<i>-4.11</i>
(510MPa, -430MPa)	281.09	0.20	+280.89
(520MPa, -440MPa)	162.60	0.29	+162.31
(540MPa, -460MPa)	46.51	0.01	+46.5
Average	86.2	4.46	+81.74

Fig. 2 presents a comparison of the (AA7075-T6) stabilised 1.5% strain controlled experimental cycle (150th cycle) with the MAFM model simulated results for the parameters obtained by baseline and optimised methods.

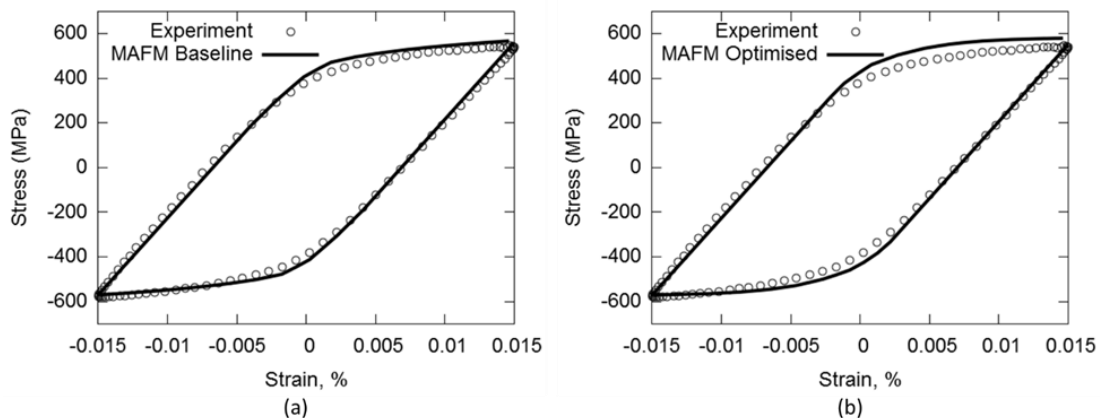


Fig. 2. AA7075-T6 hysteresis loop (150th cycle): Experimental data (circle points) and MAFM model simulated results (line) with parameters obtained in (a) baseline and (b) optimised calculation methods.

A comparison between three different levels of mean stress relaxation test data with simulation results are given in Fig. 3.

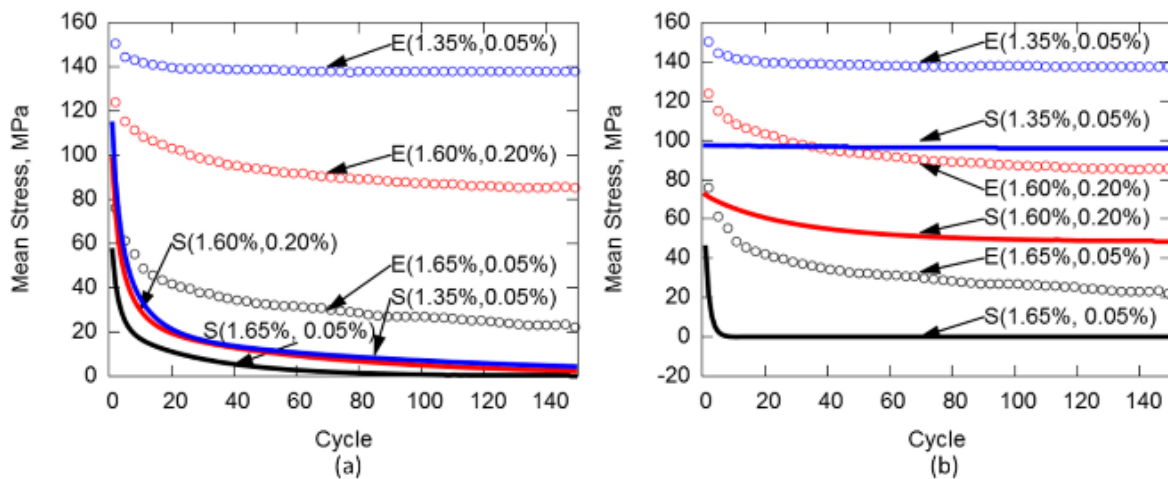


Fig. 3. AA7075-T6 mean stress relaxation: Experimental data (circle points) and MAFM model simulated results (lines) with parameters obtained in (a) baseline and (b) optimized calculation methods.

Significant improvement was achieved by the optimised set of parameters, as indicated by the ability of the simulation results to successfully improve the level of mean stress relaxation saturation. However, the rate of evolution in relaxation of the mean stress was not improved as

successfully, which is indicated by blue and black simulated relaxation curves reaching saturation considerably faster than the experimental results.

A comparison between the test data for ratcheting and the simulation results is given in Fig. 4.

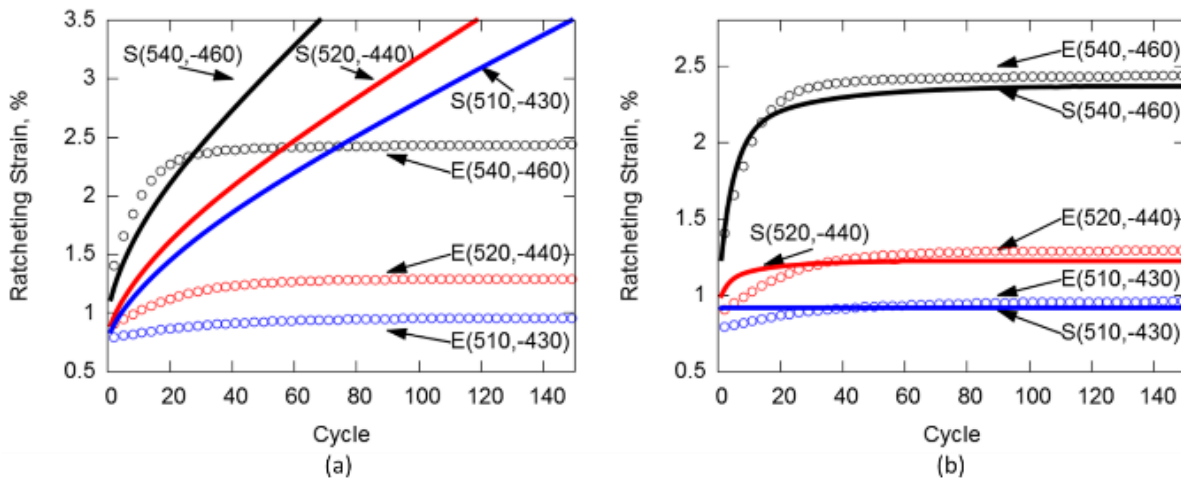


Fig. 4. AA7075-T6 ratcheting: Experimental data (circle points) and MAFM model simulated results (line) with parameters obtained in (a) baseline and (b) optimised calculation methods.

Ratcheting strain was calculated as the strain at the peak stress of each cycle. Once again, significant improvement was achieved by the optimised set of parameters. The plastic shakedown, which is seen as the stabilisation of the hysteresis loop shape due to a diminishing rate of plastic accumulation with repeated cycles, was accurately simulated in all three load cases. The strain at which the plastic shakedown occurred was accurately simulated in all three load cases using the optimised set of parameters. This is an improvement on the baseline parameter simulation which were incapable of predicting plastic shakedown in any of the tested load cases.

Comparing the baseline and optimized simulation results, it has been shown that improved results are obtained for mean stress relaxation and separately for ratcheting but not both simultaneously. This can be partially attributed to the nature of the optimisation exercise itself, which is to achieve a simulation balance between very different load cases (stress / strain controlled, under different stress and strain levels). Moreover, given the emphasis of the MAFM model on ratcheting prediction (this feature was incorporated in this model by design), better

performance is anticipated (and indeed achieved with parameter optimisation) for the corresponding cases, as opposed to mean stress relaxation.

Parameter Selection Influence

The optimisation process was further utilised to investigate the contribution of each of the MAFM model parameters in the simulation accuracy. In particular, starting from the baseline parameters, one parameter at a time was allowed to vary while the others remained constant. A least square fit of the simulated data to the experimental data was performed for each parameter variation. This resulted in a total fitness value across each objective for the stabilised hysteresis loop shape, mean stress relaxation rate and ratcheting rate. This procedure provided a means of assessing how the adjustment of one parameter influences the simulation accuracy of an alternate simulation output.

Using these results, it was found that the most influential parameter for the simulation of all cases examined (stabilised hysteresis loop, mean stress relaxation and ratcheting) was γ_i ($i = 1,2,3,4$). Ranges over which these parameters improved simulation accuracy were compared with the other parameter ranges in order to identify any overlaps. An overlap suggests that adjustment of that parameter would lead to improved simulation accuracy of all objectives. The obtained results for this comparison are shown in Fig. 5, where the different shades correspond to whether the parameter adjustment led to: improved simulation accuracy (positive), inaccurate simulations (negative), or slightly inaccurate simulations (slight negative). Values outside of the ranges displayed are not included since adjustment would result in violation of the Eq. 6 restriction.

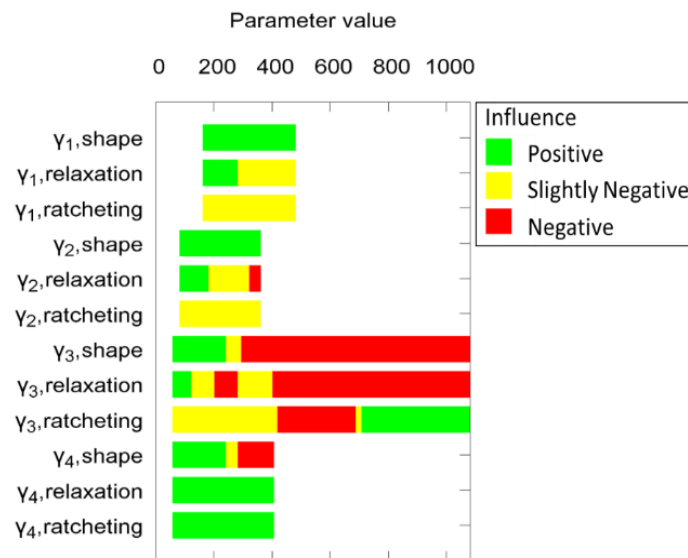


Fig.5. Comparison of the MAFM model parameters' ranges influence in simulation accuracy for hysteresis loop shape (shape), mean stress relaxation (relaxation) and ratcheting.

It is noticeable in Fig. 5 that an overlap exists in the adjustment of γ_4 (range up to 400) between shape, relaxation, and ratcheting. Effectively, improvements to simulation accuracy can be achieved for all cases by altering this parameter. Alternatively, there is a particular range (value over 600) where the variation of γ_3 will improve ratcheting, but will result in inaccurate hysteresis loop shape and mean stress relaxation simulations. The term γ_3 corresponds to the back stress having a linear-type response (low slope and very quick saturation), utilised primarily for adjusting the ratcheting rate. Thus, this term (γ_3) has the potential to influence negatively the hysteresis loop shape and relaxation, which is indeed confirmed by the sensitivity analysis. Although this inverse proportionality overlap is also noticed in γ_2 , the range over which this exists is significantly smaller (value up to 400).

Finally, there is an improvement overlap ~~in~~-existing between shape and relaxation accuracy (around the 200 value). However, varying this parameter will have a detrimental effect on ratcheting accuracy. Therefore, based on this analysis, it is recommended to adjust γ_1 , γ_2 and γ_4 when using the MAFM model, in order to achieve an improved simulation. It is also noted that, a more accurate solution could be obtained through the adjustment of γ_3 , however the inverse proportionality makes successful adjustment of this parameter very difficult.

Strain-life simulations

The optimisation method presented above provides a rational way of deriving a more robust set of parameters capable of characterising asymmetric strain-controlled and stress-controlled cyclic transient behaviour for varying loading conditions. In order to illustrate the importance of parameter selection on fatigue life prediction, the MAFM was implemented in the Defence Science and Technology (DST) Group developed fatigue analysis program called CGAP (Wallbrink and Hu, 2010) and used in strain-life fatigue calculations. Assessment of the performance of the model defined using the baseline and optimised parameters was conducted using past experimental data gathered as part of the P-3C Orion aircraft service life assessment program performed at DST Group (Mongru et al., 2010, Matricciani et al., 2016). Strain-life fatigue calculations were conducted for 21 different load spectra, using the baseline and optimised parameters, and compared to the prior experimental data gathered from notched coupons. The fatigue calculation process is summarised as following:

- In the strain-life fatigue calculation method the Neuber's rule (Neuber, 1961) was used to relate the remote stress to local stress and strains.
- The equivalent strains, used in conjunction with the strain-life curve, were calculated using the modified Morrow equation (Dowling, 2009).
- Finally, fatigue damage accumulation was calculated using Miner rule (Miner, 1945).

Simulation results using the baseline and optimised parameter sets are compared in Fig. 6, directly to the geometric mean calculated using the experimental fatigue lives gathered for each of the 21 load spectra. A majority of both simulation groups (baseline and optimised) are contained in the lower (green shaded) portion of the chart, which indicates that most of the simulations are conservative.

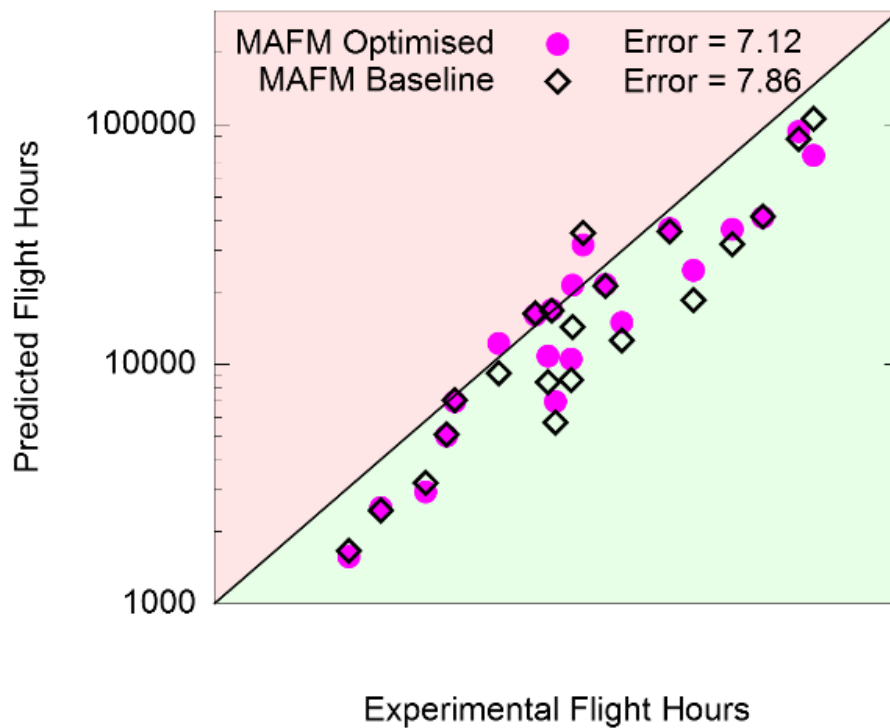


Fig. 6. *Simulated fatigue lives plotted against the corresponding geometric mean of the experimental results.*

Given on Fig. 6 is the accumulated difference for the MAFM optimised and baseline fatigue simulations. The results compare the geometric mean of the experimental data for each spectrum with the simulated fatigue life, as calculated using Eq. 8 with $M = 21$.

The total accumulated error across all 21 spectra is lower for the optimised MAFM simulations, indicating an improvement to strain-life fatigue calculations. To provide a closer inspection of the improvement for each of the spectra tested, Fig. 7 compares the calculated difference between the predicted value using the MAFM optimised and MAFM baseline to the geometric mean of the experimental data for each spectrum.

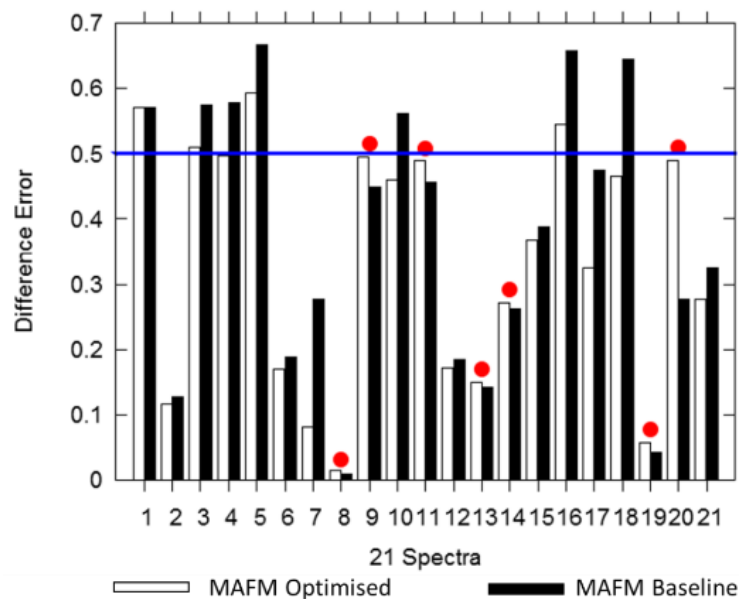


Fig. 7. *Difference in predicted and geometric mean for each of the 21 tested spectra.*

What is conveyed by examining Fig. 7 is the improvement in fatigue accuracy. The blue line drawn at 50% error highlights how the optimised parameters have reduced the tested spectra with errors greater than 50% from 7 to 4. Overall, the fatigue accuracy has been improved in 14 of the tested spectra. The 7 tested spectra which do not provide an improvement in results are indicated by the red dots on top of the graph bars. However, out of the 7 cases, where the optimised parameters do not offer an improvement, the results are still very much comparable to the MAFM baseline simulations.

Discussion

It is observed that the optimised parameters have resulted in a slight decrease in the simulation accuracy of the stabilised strain-controlled hysteresis loop (Fig. 2), when compared to the baseline parameters as demonstrated by the larger error calculation for the optimised parameter simulation. This reduction in accuracy can be explained with reference to the optimisation procedure. The parameter search in the optimisation spans multiple objectives and the narrowing of the search across the population of potential solutions is aimed at achieving comparable accuracy for all objectives. This could result in a reduction in accuracy in some of the objectives in order to provide a more robust parameter set for a wider range of loading conditions, which

explains the slight reduction in accuracy in the optimised MAFM symmetric strain-controlled simulations.

The optimisation process had difficulty in accurately simulating both the ratcheting and mean stress relaxation phenomena in strain-controlled load cases which do not induce complete relaxation of the mean stresses. The model was considerably more capable of accurately simulating the ratcheting behaviour than the mean stress relaxation behaviour. This is further supported by Fig. 8 where the ratcheting and mean stress relaxation objectives are plotted for all valid iterations.

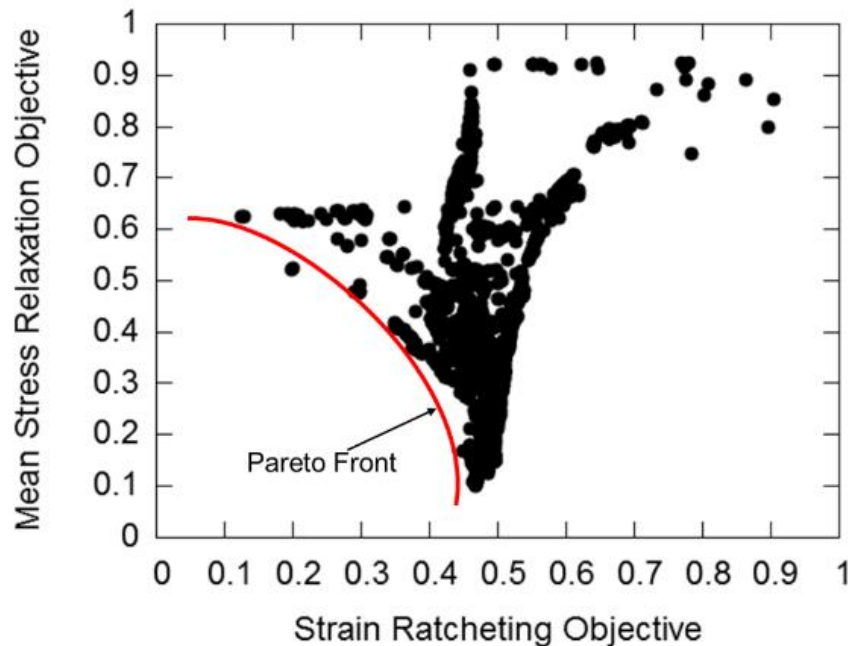


Fig. 8. *Evolution of multi-objective design iterations (mean stress relaxation versus strain ratcheting objectives).*

Fig. 8 was constructed from results gathered from a multi-objective analysis using three objectives: (1.5%,-1.5%) stabilised hysteresis loop, (540MPa,-460MPa) ratcheting strain, and (1.6%, 0.2%) mean stress relaxation. The smaller number of objectives was utilised in order to more effectively investigate the relationship between the accuracy in mean stress relaxation and ratcheting simulations. Indicated in Fig. 8 is what is known as the Pareto front, which gives an understanding of the trade-off that exists between objectives. Optimisation to improve accuracy

for mean stress relaxation leads to a reduction in accuracy for ratcheting, and vice versa. At the midpoint of this front the two objective values are comparable; therefore, although the simulation accuracies for both objectives are comparable neither objective has been completely optimised. The shape of the Pareto front also provides an understanding of the relationship between objectives. The concave appearance of the Pareto front suggests a very strong trade-off between objectives; therefore, the existence of significant conflicting simulation accuracy between ratcheting and mean stress relaxation.

The strain-life fatigue application using the optimised parameters highlighted the importance of using an optimisation procedure to develop a more robust parameter set capable of simulating a variety of different cyclic transient phenomena. This was indicated by the improvement in the accuracy of fatigue life prediction for the majority of aircraft service loads tested. This improvement in accuracy also highlighted the potential of using uniaxial constant amplitude experimental data to develop kinematic and isotropic hardening parameters to be used in the strain-life fatigue analysis which implements complex variable amplitude loading.

Conclusions

Current engineering practice is generally limited to using plasticity models embedded within commercial finite element analysis packages (i.e. MAF model), which are known to have performance limitations. The simulation results presented in this study highlight the significant benefit of employing an optimisation procedure to determine the parameters for the advanced MAFM model. This is an important finding from the point of view of applied engineering, since sophisticated plasticity models (such as MAFM) can be employed more accurately by properly selecting (optimising) their parameters.

The simulation accuracy of cyclic phenomena occurring from a number of different loading cases was drastically improved with the application of a multi-objective optimisation method (included in the mode-Frontier software), in comparison to the standard protocols used for the determination of model parameters. The optimisation method was successfully employed to provide a better understanding of the influence that each of the different MAFM model parameters has on the overall simulation accuracy. This implementation exercise has confirmed the suitability of an optimisation process available in commercial software, which is accessible

Post-print: Dylan Agius, Mladenko Kajtaz, Kyriakos I. Kourousis, Chris Wallbrink, Weiping Hu, (2018) "Optimising the multiplicative AF model parameters for AA7075 cyclic plasticity and fatigue simulation", Aircraft Engineering and Aerospace Technology, Vol. 90 Issue: 2, pp.251-260, <https://doi.org/10.1108/AEAT-05-2017-0119>

by engineers working on structural analysis and does not require specialist knowledge in the mathematical background, formulation and numerical algorithms involved.

Moreover, the optimisation identified an issue associated with competing ratcheting and mean stress relaxation objectives; highlighting the issues associated with arriving at a parameter set which can accurately simulate ratcheting and mean stress relaxation for strain-controlled load cases incapable of inducing complete relaxation. This finding can be useful when researchers and engineers employ advanced plasticity models (in the examined case the MAFM model) for problems requiring a more focused parameter selection strategy (i.e. if ratcheting is the main concern in a structural problem, the parameters' variation window can be adjusted accordingly, etc).

Finally, the importance of parameter optimisation based on uniaxial stress/strain-controlled phenomena was demonstrated through the application of the MAFM optimised and baseline models to strain-life fatigue calculations. Again, from the standpoint of an overall improved performance (low and high cycle fatigue simulation), this analysis illustrated that advanced plasticity modelling can have a positive influence through a time efficient optimisation exercise.

Focused research on the use of advanced plasticity models can be very useful in engineering practice, where time and simplicity is of outmost importance. This study is considered a valuable contribution for the engineering community, as it can act as starting point for further exploration of the benefits that can be obtained through material parameter optimisation methodologies for models of the MAF class.

Acknowledgments

The financial support of the Defence Science and Technology Group (DSTG) of the Australian Department of Defence (DSTO-RMIT Research Agreement ref. 2014/1032188/1) is acknowledged.

References

Agius, D., Kajtaz, M., Kourousis, K. I., Wallbrink, C., Wang, C. H., Hu, W. & Silva, J. (2017a), "Sensitivity and optimisation of the Chaboche plasticity model parameters in strain-life fatigue predictions", *Materials & Design*, Vol. 118, pp. 107-121.

Agius, D., Kourousis, K. I., Wallbrink, C., Hu, W., Wang, C. H. & Dafalias, Y. F. (2017b), "Aluminum Alloy 7075 Ratcheting and Plastic Shakedown Evaluation with the Multiplicative Armstrong–Frederick Model", *AIAA Journal*, Vol.55, No.7, pp. 2461-2470.

Alt, H. & Godau, M. (1995), "Computing the Frechet Distance Between Two Polygonal Curves".*International Journal of Computational Geometry & Applications*, Vol. 05, pp. 75-91.

Armstrong, P. J. & Frederick, C. O. (1966), "A Mathematical Representation of the Multiaxial Bauschinger Effect", *G.E.G.B. Report RD/B/N*. Central Electricity Generating Board.

Badnava, H., Pezeshki, S. M., Fallah Nejad, K. & Farhoudi, H. R. (2012), "Determination of combined hardening material parameters under strain controlled cyclic loading by using the genetic algorithm method", *Journal of Mechanical Science and Technology*, Vol. 26, pp. 3067-3072.

Bari, S. & Hassan, T. (2000), "Anatomy of coupled constitutive models for ratcheting simulation", *International journal of plasticity*, Vol. 16, pp. 381-409.

Cermak, M., Halama, R., Karasek, T. & Rojicek, J. "Parameter identification of chaboche material model using indantation test data and inverse approach", in *COUPLED PROBLEMS 2015 - Proceedings of the 6th International Conference on Coupled Problems in Science and Engineering, 2015*, pp. 743-752.

Chaboche, J. L. (1986), "Time Independent Constitutive Theories for Cyclic Plasticity", *International Journal of plasticity*, Vol. 2, pp. 493-496.

Chaboche, J. L. (1991), "On some modifications of kinematic hardening to improve the description of ratchetting effects", *International Journal of Plasticity*, Vol. 7, pp. 661-678.

Post-print: Dylan Agius, Mladenko Kajtaz, Kyriakos I. Kourousis, Chris Wallbrink, Weiping Hu, (2018) "Optimising the multiplicative AF model parameters for AA7075 cyclic plasticity and fatigue simulation", *Aircraft Engineering and Aerospace Technology*, Vol. 90 Issue: 2, pp.251-260, <https://doi.org/10.1108/AEAT-05-2017-0119>

Chaboche, J. L., Dang-Van, K. & Cordier, G. "Modelization of the strain memory effect on the cyclic hardening of 316 stainless steel", in *Fifth International Conference on SMiRT, Berlin, Germany, 1979*

Chaparro, B. M., Thuillier, S., Menezes, L. F., Manach, P. Y. & Fernandes, J. V. (2008), "Material parameters identification: Gradient-based, genetic and hybrid optimization algorithms", *Computational Materials Science*, Vol. 44, pp. 339-346.

Dafalias, Y. F., Kourousis, K. I. & Saridis, G. J. (2008), "Multiplicative AF kinematic hardening in plasticity", *International Journal of Solids and Structures*, Vol. 45, pp. 2861-2880.

Desai, C. S. & Chen, J. Y. (2006), "Parameter optimization and sensitivity analysis for disturbed state constitutive model", *International Journal of Geomechanics*, Vol. 6, pp. 75-88.

Dowling, N. E. (2009), "Mean stress effects in strain–life fatigue", *Fatigue & Fracture of Engineering Materials & Structures*, Vol. 32, pp. 1004-1019.

Esteco 2015. ModeFrontier. In. <http://ww.esteco.com>.

Farrahi, G. H., Shamloo, A., Felfeli, M. & Azadi, M. (2014), "Numerical simulations of cyclic behaviors in light alloys under isothermal and thermo-mechanical fatigue loadings", *Materials and Design*, Vol. 56, pp. 245-253.

Franulović, M., Basan, R. & Prebil, I. (2009), "Genetic algorithm in material model parameters' identification for low-cycle fatigue", *Computational Materials Science*, Vol. 45, pp. 505-510.

Furukawa, T., Sugata, T., Yoshimura, S. & Hoffman, M. (2002), "An automated system for simulation and parameter identification of inelastic constitutive models", *Computer Methods in Applied Mechanics and Engineering*, Vol. 191, pp. 2235-2260.

Grama, S. N., Subramanian, S. J. & Pierron, F. (2015), "On the identifiability of Anand viscoplastic model parameters using the Virtual Fields Method", *Acta Materialia*, Vol. 86, pp. 118-136.

Post-print: Dylan Agius, Mladenko Kajtaz, Kyriakos I. Kourousis, Chris Wallbrink, Weiping Hu, (2018) "Optimising the multiplicative AF model parameters for AA7075 cyclic plasticity and fatigue simulation", *Aircraft Engineering and Aerospace Technology*, Vol. 90 Issue: 2, pp.251-260, <https://doi.org/10.1108/AEAT-05-2017-0119>

Hu, W., Wang, C. H. & Barter, S. (1999), Analysis of Cyclic Mean Stress Relaxation and Strain Ratchetting Behaviour of Aluminium 7050, *Report DSTO0-RR-153*, Melbourne, Defence Science and Technology Organisation.

Hu, W. P. & Wallbrink, C. "Fatigue life analysis of specimens subjected to infrequent severe loading using a nonlinear kinematic hardening cyclic plasticity model", *11th International Fatigue Congress, FATIGUE 2014 in Melbourne, Australia*, Advanced Materials Research, Vol. 891-892, pp. 512-517.

Khademi, E., Majzoobi, G. H., Bonora, N. & Gentile, D.(2015), "Experimental modeling of strain-dependent cyclic plasticity for prediction of hysteresis curve", *Journal of Strain Analysis for Engineering Design*, Vol. 50, pp. 314-324.

Khutia, N. & Dey, P. P. (2014), "Material parameter optimisation of Ohno-Wang kinematic hardening model using multi objective genetic algorithm", *International Journal of Computational Materials Science and Surface Engineering*, Vol. 6, pp. 50-74.

Kourousis, K. I. & Dafalias, Y. F. (2013), "Constitutive modeling of Aluminum Alloy 7050 cyclic mean stress relaxation and ratcheting", *Mechanics Research Communications*, Vol. 53, pp. 53-56.

Krishna, S., Hassan, T., Ben Naceur, I., Saï, K. & Cailletaud, G. (2009), "Macro versus micro-scale constitutive models in simulating proportional and nonproportional cyclic and ratcheting responses of stainless steel 304", *International Journal of Plasticity*, Vol. 25, pp. 1910-1949.

Mahmoudi, A. H., Pezeshki-Najafabadi, S. M. & Badnava, H. (2011), "Parameter determination of Chaboche kinematic hardening model using a multi objective Genetic Algorithm", *Computational Materials Science*, Vol. 50, pp. 1114-1122.

Mahnken, R. & Stein, E. (1996), "A unified approach for parameter identification of inelastic material models in the frame of the finite element method", *Computer Methods in Applied Mechanics and Engineering*, Vol. 136, pp. 225-258.

Post-print: Dylan Agius, Mladenko Kajtaz, Kyriakos I. Kourousis, Chris Wallbrink, Weiping Hu, (2018) "Optimising the multiplicative AF model parameters for AA7075 cyclic plasticity and fatigue simulation", *Aircraft Engineering and Aerospace Technology*, Vol. 90 Issue: 2, pp.251-260, <https://doi.org/10.1108/AEAT-05-2017-0119>

Matricciani, E., Duthie, J. & Walker, K. (2016), DST Group P-3 FAMS/FASTRAN Recalibration Coupon Testing in Support of the 2010 Structural Management Plan Review, *DST-Goup_TR-2659*. Melbourne, Australia, Defence Science and Technology Group.

Miner, M. A. (1945), "Cumulative damage in fatigue", *Journal of Applied Mechanics*, Vol. 12, pp. A159-A164.

Mongru, D., Jackson, P., Maxfield, K. & Wallbrink, C. (2010). Evaluation of Alternative Life Assessment Approaches Using P-3 SLAP Test Results, *DSTO-TR-2418*, Melbourne, Australia, Defence Science and Technology Group.

Neuber, H. (1961), "Theory of Stress Concentration for Shear-Strained Prismatical Bodies With Arbitrary Nonlinear Stress-Strain Law". *Journal of Applied Mechanics*, Vol. 28, pp. 544-550.

Poloni, C. & Pediroda, V. (1997). "GA coupled with computationally expensive simulations: tools to improve efficiency". In: *Genetic Algorithms and Evolution Strategy in Engineering and Computer Science*. pp. 267-288. John Wiley & Sons, Chichester, UK.

Rahman, S. M., Hassan, T. & Ranji Ranjithan, S. "Automated parameter determination of advanced constitutive models", in *American Society of Mechanical Engineers, Pressure Vessels and Piping Division (Publication) PVP, 2005*, pp. 261-272.

Rokonuzzaman, M. & Sakai, T. (2010), "Calibration of the parameters for a hardening–softening constitutive model using genetic algorithms", *Computers and Geotechnics*, Vol. 37, pp. 573-579.

Saleeb, A. F., Gendy, A. S. & Wilt, T. E. (2002), "Parameter-estimation algorithms for characterizing a class of isotropic and anisotropic viscoplastic material models", *Mechanics Time-Dependent Materials*, Vol. 6, pp. 323-362.

Sinaie, S., Heidarpour, A. & Zhao, X. L. (2014), "A multi-objective optimization approach to the parameter determination of constitutive plasticity models for the simulation of multi-phase load histories", *Computers and Structures*, Vol. 138, pp. 112-132.

Post-print: Dylan Agius, Mladenko Kajtaz, Kyriakos I. Kourousis, Chris Wallbrink, Weiping Hu, (2018) "Optimising the multiplicative AF model parameters for AA7075 cyclic plasticity and fatigue simulation", *Aircraft Engineering and Aerospace Technology*, Vol. 90 Issue: 2, pp.251-260, <https://doi.org/10.1108/AEAT-05-2017-0119>

Wallbrink, C. & Hu, W. (2010). A Strain-Life Module for CGAP: Theory, User Guide and Examples. *DSTO-TR-2392*, Melbourne, Australia, Defence Science and Technology Organisation.

Yun, G. J. & Shang, S. (2011), "A self-optimizing inverse analysis method for estimation of cyclic elasto-plasticity model parameters", *International Journal of Plasticity*, Vol. 27, pp. 576-595.

Zhao, K. M. & Lee, J. K. (2002), "Finite element analysis of the three-point bending of sheet metals", *Journal of Materials Processing Technology*, Vol. 122, pp. 6-11.